FEBS Letters 589 (2015) 2117–2123

FEBS Letters

journal homepage: www.FEBSLetters.org

Double stranded promoter region of BRAF undergoes to structural rearrangement in nearly physiological conditions

Maria Laura Greco [a], Marco Folini [b], Claudia Sissi [a,*]

[a] Dept. of Pharmaceutical and Pharmacological Sciences, v. Marzolo 5, 35131 PD, Italy
[b] Dept. of Experimental Oncology and Molecular Medicine, Fondazione IRCCS Istituto Nazionale dei Tumori, Via Amadeo 42, Milano, Italy

ARTICLE INFO

Article history:
Received 17 February 2015
Revised 10 June 2015
Accepted 19 June 2015
Available online 2 July 2015

Edited by Angel Nebreda

Keywords:
BRAF
G-quadruplex
i-motif
Oncogene

ABSTRACT

The folding of oncogene promoters into non-canonical DNA secondary structures is considered a strategy to control gene expression. Herein, we focused on a 30 bases sequence located upstream of the transcription start site of *BRAF* (Braf-176) that contains 80% of guanines. We analyzed the structural behavior of the G- and C-rich strands. By the use of spectroscopic and electrophoretic techniques we confirmed that they actually fold into a predominant antiparallel G-quadruplex and into an i-motif, respectively, and that they can coexist at nearly physiological conditions. Finally, the influence of several factors (KCl, pH, PEG_{200}) on the conversion of the double stranded form of the oncogene promoter into the two above mentioned non-canonical structures has been explored.

1. Introduction

In the last two decades, the potential connection between G-rich nucleic acid sequences and modern chemotherapy has been the object of several studies. The peculiarity of these sequences is related to their attitude to fold into G-quadruplex structures (G4), tetrahelical tridimensional arrangements supported by the overlapping of planar arrays formed by four guanines paired together by a network of Hoogsten bonds [1]. These structures can form at the telomeric end of chromosomes but also in the promoter region of genes and within the 5′ untranslated region (5′ UTR) of mRNAs [2–5] and their involvement in replication and transcription is now well assessed [6]. Indeed, these mechanisms are finely tuned through the recruitment of many proteins at specific promoter sites where the DNA/RNA–protein interactions are profoundly influenced by the structural arrangement(s) of the nucleic acid. Thus, the predominance of one structure over the others determines an additional switching on/off mechanism [7]. Surprisingly, the large majority of the putative G-quadruplex forming (PQF) sequences turned out to be preferentially located in the promoters of proto-oncogenes and transcription factors rather than in tumor suppressor or housekeeping genes thus foreseeing a functional role of G4 structures as a switch-off element for gene transcription [8]. Consistently, gene silencing by G4 stabilization has been considered as a valuable alternative to the nucleic acid-based approaches currently used in cellular systems (e.g., antisense oligomers, siRNA) [9–11].

Up-to-date, the promoter sequences of several oncogenes have been investigated for their ability to fold into G4 structures. Relevant examples are *c-MYC*, *KIT*, *KRAS*, *BCL-2*, *VEGF*, *PDGF-α*, *PDGFR-B* and *RET*. For some of these DNA sequences the corresponding G4 strucutres have been solved by NMR or X-ray [12–18]. Additionally, it was clearly shown that small molecules able to stabilize the G4 form of *c-MYC*, *cKIT* or *KRAS* promoters, sensibly decrease the oncogene expression at both the mRNA and protein levels in cancer cells [3,19–22].

Recently, the oncogene *BRAF* has been analyzed in terms of PQF sequences. The interest for this gene relies on its role in several cancers [23]. Indeed, it encodes for a serine-threonine protein kinase and some activating mutations (among which the BrafV600E is the most extensively studied) are seen in about 70% of primary melanomas, 10% of colorectal cancers and 30–70% of papillary thyroid carcinomas [24]. Two main G-rich sequences have been identified in the promoter region of this gene. One, named *B-raf*, is placed five bases down-stream the transcription start site (TSS) (on the opposite strand of the sequence coding for the 5′-untranslated region, 5′ UTR) and its G4 structure has been solved by X-ray spectroscopy [25]. The second one is located upstream the TSS at position −176.

Author contributions: Maria Laura Greco contributed 40%, Marco Folini 20%, Claudia Sissi 40%.

* Corresponding author.
E-mail address: claudia.sissi@unipd.it (C. Sissi).

http://dx.doi.org/10.1016/j.febslet.2015.06.025
0014-5793/

Here, we present the first evidences to support the G4 folding of the G-rich sequence of Braf-176. Additionally, we take into account that, in the cells, oncogenic sequences are in their double stranded form. Thus, the conformational study has been extended towards the complementary strand. Indeed, C-rich sequences can assume a peculiar conformation called i-motif (iM) stabilized by hydrogen bonding between the N3 of two cytosines [26,27]. Although this peculiar conformation is favoured at pH 5.0 (where cytosines are hemiprotonated) its occurrence may provide an additional perturbation of the stability of the double stranded form of the tested oncogenic sequence.

The so far acquired information have been finally applied to the double stranded system to further validate the relevance of these structural equilibria on the physiological substrate.

2. Materials and Methods

2.1. Materials

Synthetic oligonucleotides (Bioscience, Belgium) were resuspended in milliQ water and purified by PAGE before use. The tested sequences are reported in Table 1. ds_Braf-176 was obtained by annealing equimolar amounts of the two complementary strands, Braf-176 and C_Braf-176.

2.2. Circular dichroism measurements

CD spectra were recorded using 1 cm pathlength cells on a Jasco J810 spectropolarimeter equipped with a NESLAB temperature controller. Before data acquisition, DNA solutions (ca. 4 μM, strand concentration) were heated at 95 °C for 5 min and left to cool overnight at room temperature in the required buffer (10 mM Tris, 1 mM EDTA, variable KCl and pH). Each reported spectrum represents the average of 3 scans. Observed ellipticities were converted to mean residue ellipticity $[\Theta] = \text{deg} \times \text{cm}^2 \times \text{dmol}^{-1}$ (Mol. Ellip.). When required, the variation of the dichroic signal at a selected wavelength was monitored as a function of the temperature using a heating/cooling rate of 1 °C/min in the temperature range 25–95 °C. Melting temperatures were determined by the first derivative of the melting curves.

To calculate the apparent dissociation constant for KCl (K_d), the fraction of bound DNA was calculated as $(S - S_o)/(S_\infty - S_o)$, where S_o and S_∞ are the signal corresponding to free and bound DNA and S is the signal recorded at variable KCl concentration. Experimental data were fitted according to a single binding event according to the following equation: bound fraction = [KCl]/([KCl] + K_d).

2.3. Thermal differential spectrum (TDS)

Thermal difference spectra were obtained by subtracting the UV absorption spectra of tested sequences acquired at 25 °C and at 95 °C in 10 mM Tris, 100 mM KCl at the reported pH in a Perkin Elmer λ20 spectrometer. The resulting thermal difference spectra were normalized to the value of 1 at the maximal intensity.

Table 1
Sequences used in this work and corresponding melting temperatures (T_m) determined by CD[(a)] or UV[(b)] spectroscopy in 10 mM Tris, 1 mM EDTA, 100 mM KCl, pH 7.0. Error ± 0.4 °C. G–T mutations are highlighted in bold.

Sequence		T_m (°C)
Braf-176	5′-GGGGGTGCGGGGGGGAGCGGGGGAAGGGGG	90.2[(a)]
C_Braf-176	5′-CCCCCTTCCCCCGCTCCCCCCCGCACCCCC	40.6[(b)]
Braf-176_T1	5′-GGGGGTGCGGG**T**GGGAGCGGGGGAAGGGGG	90.1[(a)]
Braf-176_T2a	5′-GGGGGTGCG**TGT**GGGAGCGGGGGAAGGGGG	85.0[(a)]
Braf-176_T2b	5′-GGGGGTGCGGG**TGT**GAGCGGGGGAAGGGGG	90.0[(a)]
Braf-176_T2c	5′-GGGGGTGCG**T**GGG**T**GAGCGGGGGAAGGGGG	92.6[(a)]
Braf-176_T3	5′-GGGGGTGCG**TGTGT**GAGCGGGGGAAGGGGG	60.1[(a)]
ds_Braf-176	5′-$C_5T_2C_5GCTC_7GCAC_5$ 3′-$G_5A_2G_5CGAG_7CGTG_5$	79.0[(b)]

2.4. Electromobility shift assay (EMSA)

Single-stranded oligonucleotides were 5′-labelled with T4 polynucleotide Kinase (Thermo Scientific) and [γ^{32}P] ATP (Perkin Elmer, Life Sciences). A mixture of purified labelled and unlabelled oligonucleotides (total final concentration 1 μM) was heated to 95 °C for 5 min in 10 mM Tris, 1 mM EDTA, pH 8.0 with increasing KCl concentrations and let to cool overnight at room temperature. The folding of the starting material was monitored by native 20% polyacrylamide gel in 0.5× TBE (44.5 mM Tris, 44.5 mM boric acid and 1 mM EDTA) in the presence or absence of 10 mM KCl (11 V/cm for 2.5 h). Resolved bands were visualized on a Phosphor Imager (STORM 840, Pharmacia Biotech Amersham).

2.5. Fluorescence melting studies

Fluorescence melting experiments were performed using Braf-176 labeled with Dabcyl at the 5′-end and FAM at the 3′-end alone or previously annealed with its complementary strand. DNA solutions (0.25 μM) were prepared in 10 mM LiOH at the required pH with H_3PO_4 and added of different concentration of KCl. The resulting samples were slowly heated to 95 °C (1 °C/min) in a Roche LightCycler where the fluorescence emission was recorded at 520 nm (excitation source set at 488 nm). T_m values were determined from the first derivatives of the melting profiles using the Roche LightCycler software. Each curve was repeated at least three times and errors were ±0.4 °C.

3. Result and discussion

3.1. Folding of BRAF-176 into G-quadruplex structure(s)

The peculiarity of the identified Braf-176 sequence is related to the impressive number of guanines it contains (80%). This can easily lead to the potential formation of multiple G4 structures. To monitor the structural equilibria occurring within this sequence, we used CD spectroscopy [28]. Indeed, unique dichroic features are associated to defined tridimensional orientation of the DNA chromophores that derive from the nucleic acid secondary structure. Analyses were performed in the presence/absence of K^+, a metal ion known to promote and stabilize G4. Titration curves showed that the metal ion altered the dichroic spectrum of Braf-176 according to a process that reached saturation al low K^+ concentration (about 10 mM) with an apparent $K_d = 0.64 \pm 0.03$ mM (Fig. 1A and B). Interestingly, a good correlation between the thermal stabilization driven by the metal ion and the CD signal variation it promotes was found. Additionally, it is worth to underline that the thermal stability of Braf-176 (≈90 °C for $K^+ > 25$ mM) is much larger than the one recorded for the previously reported *B-raf* sequence located in the 5′ UTR region [25].

The variation of the optical signal induced by KCl was modest but led to a final form identified by a strong positive band centered at 295 nm and a modest negative band in the 230–250 nm range. This combination of dichroic contributions has been related to a G4 structure likely arranged into a main antiparallel folding deriving from overlapping of guanosine of alternating syn/anti glycosidic bond. This model was in line with TDS results (Fig. 1C) [29]. Moreover, EMSA analysis confirmed that KCl causes the samples to migrate faster than a linear oligonucleotide of comparable length (Fig. 1D). These evidences allowed us to propose that Braf-176 is actually able to fold into a predominant intramolecular antiparallel G4 structure.

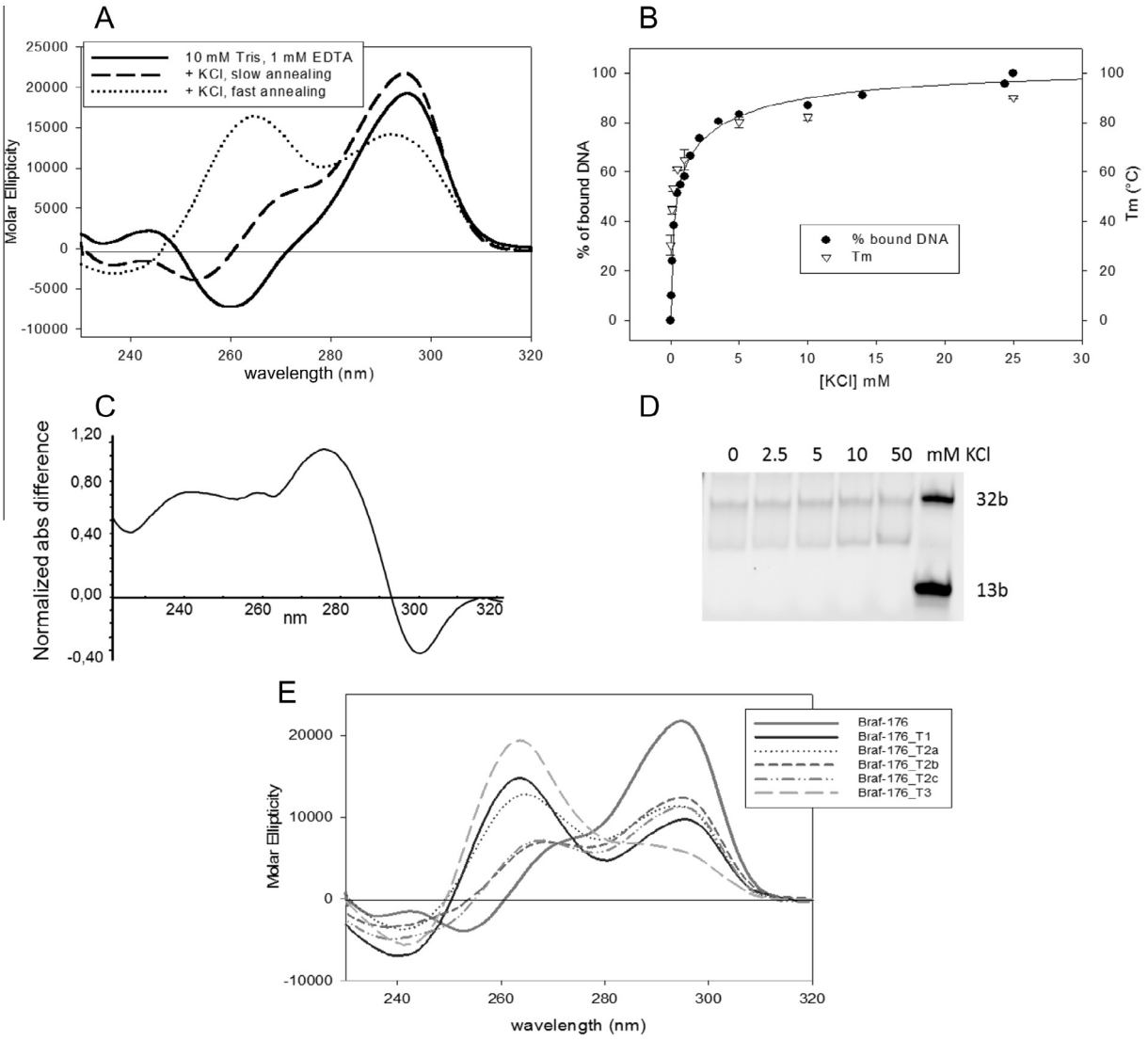

Fig. 1. CD spectra of 4 μM Braf-176 recorded in the absence (solid lines) or in the presence of 100 mM KCl in 10 mM Tris, 1 mM EDTA, pH 7.0 after a slow (1 °C/min, dashed line) or a fast (10 °C/min, dotted line) annealing step (A). The % of DNA bound by the metal ion derived from CD titrations (full circles) and the corresponding melting temperatures (empty triangles) plotted as a function of KCl concentration (B). In (C) the thermal difference spectrum corresponding to the slow annealed sample in 10 mM Tris, 1 mM EDTA, 100 mM KCl, pH 7.0 is reported whereas, in (D), the electrophoretic pattern on a 20% native polyacrylamide gel in TBE 0.5× of Braf-176 in presence of increasing KCl concentrations is shown. Markers refer to unfolded single strand sequences 32 or 13 bases long. In (E) the CD spectra of the mutated Braf-176 sequences (4 μM) annealed in 10 mM Tris, 1 mM EDTA, 100 mM KCl, pH 7.0 are reported.

Nevertheless, the potential folding of Braf-176 into G4 of different topologies was not fully excluded. Indeed, working at KCl concentrations higher than 50 mM two thermal transitions were observed. Additionally, a fast annealing step (10 °C/min) allowed trapping a CD signal characterized by a strong positive band centered at 265 nm (Fig. 1A). Since along the time, it slowly converts to the above described form, we can attribute it to a kinetically but not thermodynamically favored form.

To possibly address the bases which are responsible for the occurrence of the different G4 topologies, we acquired the CD spectrum of some Braf-176 mutants in which one, two or three G-T substitutions were introduced within the long stretch of seven adjacent guanines found in the wild type sequence (Table 1, Fig. 1E).

Generally, all tested mutants did not assume different G4 arrangements according to the annealing rate, the only exception being Braf-176_T2b which behavior resembled the one discussed for the wild type. Moreover, none of them showed an antiparallel component so relevant as Braf-176. When compared to the 260 nm band, the 295 nm contribution was still predominant for T2b and T2c but it progressively decreased in T1 and T2a up to T3 where it was almost suppressed. Surprisingly, T3 was still able to assume a G4 conformation, although characterized by a lower thermal stability. This form was characterized by an intense CD signal at 260 nm, likely deriving from the recruitment of non-consecutive Gs within a single column. Such a behavior was supported by T2a and, to a lesser extent by T1. This suggests that it is mainly the 5′ portion of the hepta-repeated sequence that is involved in driving the antiparallel component in the folding process.

3.2. Formation of G-quadruplex from ds_Braf-176

To better highlight the potential occurrance of the herein described G4 conformations of Braf-176 in cells, we investigated their formation within the corresponding double stranded fragment. The high content in GC pairs allows predicting a high stability for the double stranded too. Accordingly, by reading the

absorbance variation at 260 nm, a T_m = 85.9 °C was experimentally found in buffer that does not promote G4 formation (100 mM LiCl) (Fig. 2A). As a consequence we expect a poor tendency of the G-rich strand to dissociate from its complementary C-rich sequence to assume a G-4 conformation. Consistently, the CD spectrum of the ds_BRAF-176 acquired in the absence of KCl was not significantly affected by the subsequent addition of the G4 inducer metal ion (data not shown). This can actually derive from the modest variation associated to the G-rich strand upon K^+ binding or it can highlight a poor ability to form a G4 structure. This second hypothesis was further supported by EMSA where addition of KCl to the ds_Braf was not sufficient to cause the strand separation required in order to form G4 (Fig. 2B). However, when the two complementary strands were annealed in the presence of KCl, EMSA highlighted a significant competition between the paired B form and the G4 structure(s) (Fig. 2C). Consistently, the UV melting profile of ds_Braf-176 recorded at 260 nm, thus where the signal variation essentially derives only from the melting of the duplex, was shifted at a lower temperature when acquired in KCl containing solutions (T_m = 79.0 °C in 100 mM KCl) as a result of G4 induction (Fig. 2A, Table 1). This result was supported by a fluorescence melting assay (Fig. 2D). In this case, using the G-rich strand labelled with a fluorophore and a quencher at the 5′ and 3′ end, respectively, the fluorescence signals of the double helix, the unfolded G-rich strand and the G-4 forms are distinct and can be followed during the melting step [30]. Starting from the ds_Braf, in the absence of KCl, we observed only the transition from the double strand to the single stranded form. Conversely, when KCl was included in the reaction mixture, this step was associated to a remarkable reduction of the fluorescence signal which describes the folding of the labelled G-rich strand into a G4 structure.

By merging these data we can conclude that G4 formation can be clearly detected only upon heating the dsDNA at a temperature higher or close to its T_m and by including a KCl concentration sufficient to stabilize the tetrahelix to a larger extent. This corresponds to [KCl] higher than 5 mM (where the T_m is about 75 °C and 69 °C for the G4 and the double strand, respectively). In these conditions, the preferential stabilizing effect of the metal ion on the G4 in comparison to the ds_Braf shifted the equilibrium toward the tetrahelix that can be thus detected although non-physiological temperatures are required. Nevertheless, we must take into account that, in cell, transient lowering of the stability of the double helix can be further promoted by other events like structural stress of the double helix, helicases, etc.

3.3. Structural equilibria of C_Braf-176

In the above section, we described the competition between the double helix and G4 as the result of a balance of the relative stabilities of the two structures. However, a relevant contribution to the promotion of the tetrahelix can derive from the C-rich strand. Indeed, as above mentioned, it can be involved in the formation of an iM, although prevalently in acidic conditions. The CD spectrum of C_Braf-176 acquired at pH 5.0 was characterized by an intense dichroic band at 288 nm and a small negative band at 260 nm (Fig. 3A). Moreover, TDS recorded in the same experimental conditions showed a maximum centered at 239 nm and a minimum at 295 nm (Fig. 3B). Both these signatures are characteristic of the presence of an iM. UV melting analysis indicated it as a very stable iM with a $T_m \approx 90$ °C (Fig. 3C) and containing about 7 C—C+ pairs [31,32].

Consistently, CD spectra recorded at variable pH showed a remarkable dependence of the folded fraction with the cytosine protonation state. In fact, as it can be appreciated in Fig. 3A, the intensity of the dichroic bands progressively decreased by lowering the pH to 3.0 as a consequence of the fully protonated state

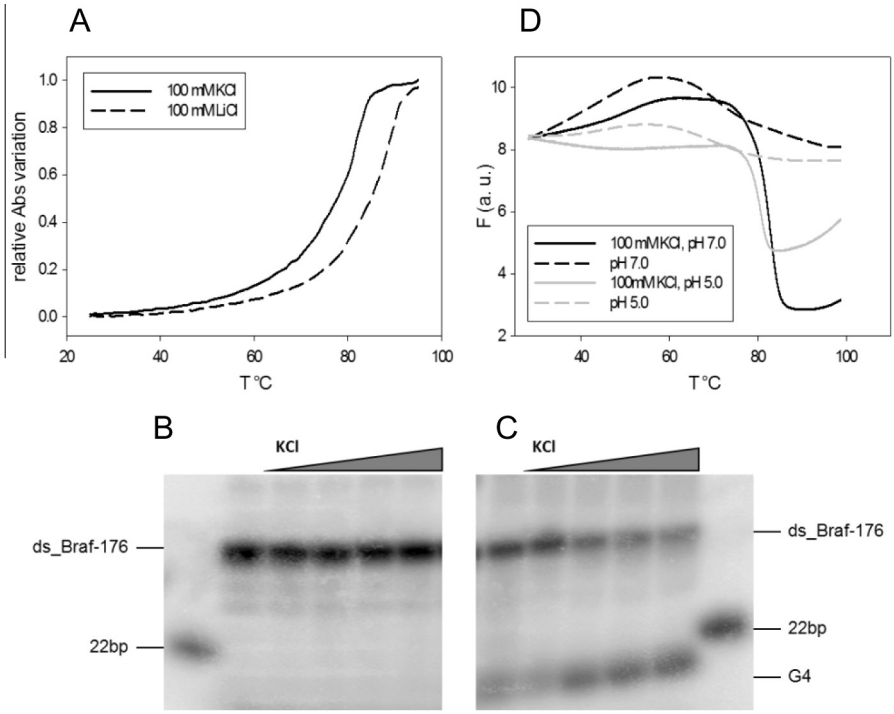

Fig. 2. Thermal denaturation profile of ds_Braf-176 recorded by UV absorbance at 260 nm in 10 mM Tris, 1 mM EDTA, pH 7.0 containing 100 mM KCl (solid line) or 100 mM LiCl (dotted line) (A). Induction of G4 structures from ds_Braf-176 by increasing concentrations of KCl (0–50 mM). Samples were loaded on a 20% native polyacrylamide gel in TBE 0.5× containing 10 mM KCl before (B) and after (C) an annealing step in the presence of the metal ion. 22 bp refers to a random sequence of 22 base pairs. In (D) the melting profiles of 0.25 μM ds_Braf-176, containing a labelled G-rich strand, in the presence (solid lines) or absence (dashed lines) of 100 mM KCl at pH 7.0 (black lines) or at pH 5.0 (gray lines) are reported.

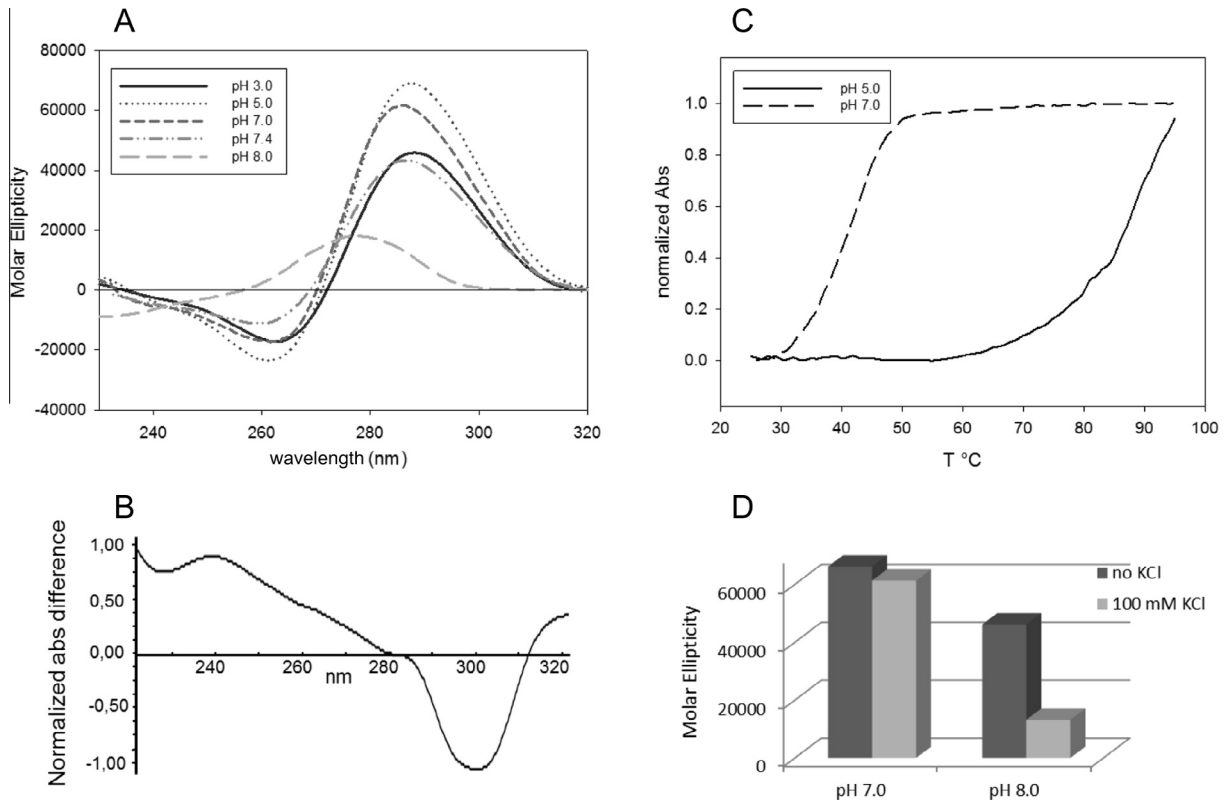

Fig. 3. CD spectra of 4 μM C_Braf-176 recorded in 10 mM Tris, 1 mM EDTA, 100 mM KCl at different pH (A), TDS corresponding to the sample at pH 5.0 (B) and melting profiles recorded at pH 7.0 and 5.0 by UV absorbance readings at 265 nm (C). In (D) the effect of 100 mM KCl on the molar ellipticity recorded at 288 nm is reported.

of cytosines which repulse one to each other thus weakening the pairing. As expected, an even more dramatic effect was observed by increasing pH up to 8.0 where the secondary structure appears to be completely lost. Likely, the spectra recorded at intermediate pH values correspond to a combination of unfolded and partially folded structures [33,34]. The interesting result that emerged from this analysis is the persistence of the iM at a nearly physiological pH value (pH 7.0). This was supported by UV melting analysis at pH 7.0 where the thermal transition occurred at 40.6 °C, a temperature higher than the physiological one (Fig. 3C, Table 1). Moreover, whereas the presence of KCl causes an extensive loss of the iM content at pH 8.0, no relevant effects on the secondary structure of C_Braf-176 were observed at pH 7.0 (Fig. 3D, S1). This led us to conclude that iM and G4 may indeed coexist.

3.4. Effect of pH or PEG_{200} on the non-canonical structures formation by ds_Braf-176

From the above data, we should expect that the stability of the ds_Braf-176 should be impaired in acidic condition as a result of the promotion of the iM. By monitoring the melting profile of ds_Braf-176 we actually observed a reduction of the temperature at which the conversion from the double stranded into the G4 occurs by shifting the working buffer from pH 7.0 to pH 5.0 (Fig. 2D). However this variation was modest (≈ 2 °C), thus making difficult to actually relate it to the concomitant iM formation rather than to a direct destabilization of the double helix due to the acidic conditions.

In order to assess if other physiologically relevant elements can further modulate these equilibria, we take into account the potential role of the crowding conditions which mimic the high nucleic acid and proteins concentration found in the nucleus. Here, we used PEG which has a well stated role in stabilizing G4 structures preferentially into a parallel conformation (Fig. 4A) [35,36]. Although it is now assessed that this is mainly due to a preferential interaction of the polymer with a defined G4 conformation rather than to excluded volume effects, we used PEG_{200} since it is one of the most used conformational transition inducer both on G4 and iM [37,38].

The dichroic spectrum of Braf-176 annealed in 100 mM KCl was not influenced by the addition of 40% (w/v) PEG_{200} confirming a high contribution of the antiparallel structure. However, when the sequence was annealed in the presence of the polymer, irrespectively of the applied cooling rate, the band centered at 295 nm (usually related to an antiparallel component) consistently decreased and one at 260 nm (parallel contribution) appears. Thus, PEG_{200} can actually provide the rearrangement of Braf-176 towards a parallel G4 arrangement. This is consistent with data on other G-rich sequences such as the human telomeric sequence for which the hybrid G4 form assumed by in KCl shifts towards a parallel G4 conformation in the presence of 40% PEG_{200} [39].

Recently, studies on the mutual influence of pH, crowding and dehydrating agents on iM have been performed too and they showed the potential of PEG to stabilize iMs up to pH 6.5 [40,41]. Working on C-Braf-176, we observed that at the lower tested pHs (5.0 and 3.0), PEG_{200} reduced the CD signal corresponding to the iM thus indicating a decrease of the folded fraction (Fig. 4B). This can be probably due to inappropriate PEG/pH balance, which leads to an increase of the electrostatic repulsion between the cytosine pairs as a result of the reduced dielectric constant for the water/PEG mixture. Of note, at pH 7.0, where the charge on cytosines is largely reduced, the CD spectrum recorded in the presence of 40% PEG_{200} showed the same signature of the iM observed at pH 5.0 (Fig. 4B, S2). This supports that crowding conditions can stabilize this conformation at pH values close to the physiological one.

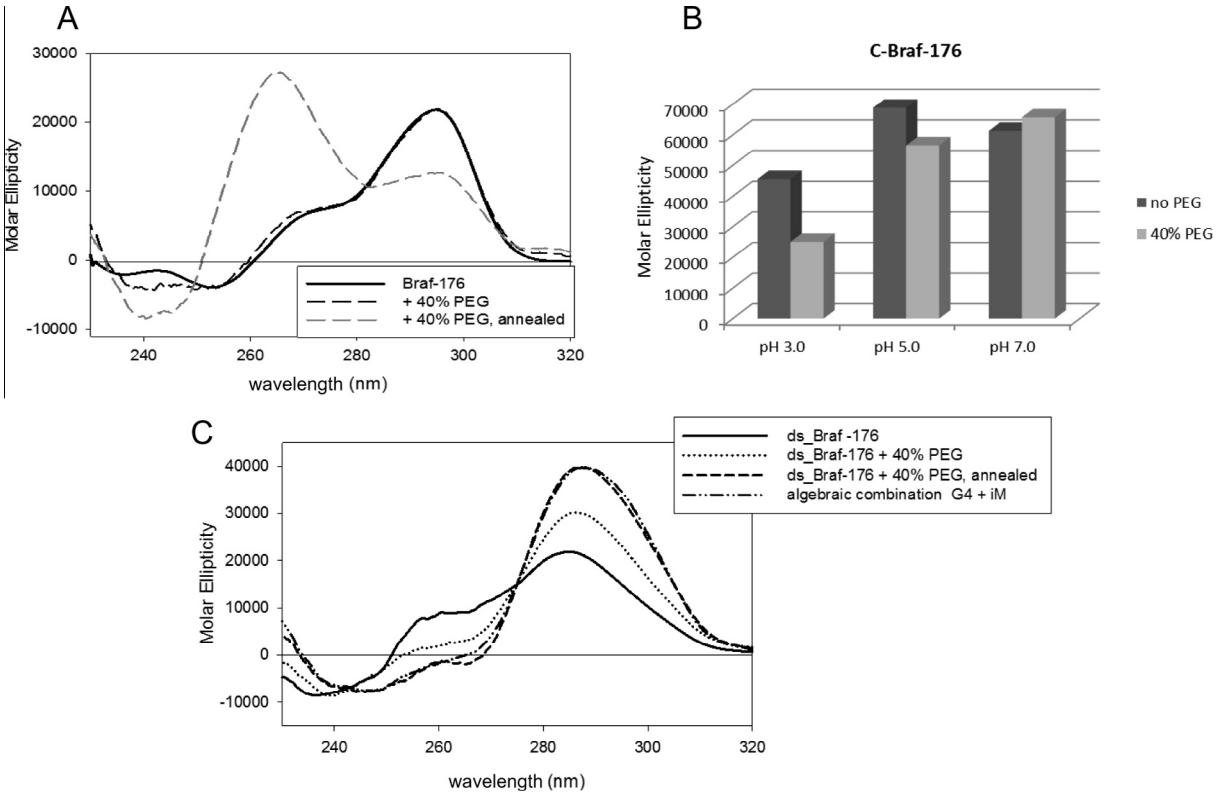

Fig. 4. CD spectra of 4 μM Braf-176 recorded in 10 mM Tris, 1 mM EDTA, 100 mM KCl, pH 7.0 (solid line) after addition of 40% PEG_{200} (black dashed line) and the annealed solution (1 °C/min, gray dashed line) (A). Molar ellipticity recorded at 287 nm of 4 μM C_BRAF-176 in 10 mM Tris, 1 mM EDTA, 100 mM KCl at different pHs, in the presence/absence of 40% PEG_{200} (B). In (C), CD spectra of 4 μM ds_BRAF-176 recorded in 10 mM Tris, 1 mM EDTA, 100 mM KCl, pH 7.0 (solid line) and after addition of 40% PEG_{200} (dotted line). Dashed line corresponds to the PEG containing sample after a slow annealing step (cooling rate 1 °C/min). The dashed-dotted line corresponds to the algebraic sum of the spectra of the G-rich and C-rich strands annealed in the same experimental conditions.

This evidence prompted us to monitor the structural equilibria of the double stranded ds_Braf-176 in the presence of PEG_{200}, too. Distinctly from what observed upon addition of only KCl, the simultaneous use of the metal ion and the polymer perturbed the structural features of the double helix leading to an increment of the dichroic band at 280 nm. Interestingly, it reached a maximum after an annealing step. It is significant to underline that this signature perfectly matches the one obtained by combining the contributions of both folded G- and C-rich strands. This allows proposing a favorable role of PEG_{200} in the conversion of the double helix towards the G4 and iM structures.

4. Conclusions

From data herein presented, we can conclude that Braf-176, thanks to its peculiar base composition, has a high potential to assume non-canonical secondary structures in physiological conditions. In particular, low potassium concentrations are sufficient to convert the G-rich Braf-176 into a predominant antiparallel G4 structure. A comparison with the available data for the previously reported *B-raf* sequence located in 5′-UTR region is interesting [25]. Indeed, in addition to the different main G4 topologies (antiparallel and parallel for B-raf and Braf-176, respectively), Braf-176 does not prefer to form G4-dimer in solution. Thus, our target can be present within one single gene copy, making it a good novel potential drug target.

At physiologically relevant KCl concentrations (100 mM) the G4 folded form of Braf-176 shows a remarkably high thermal stability ($T_m \approx 90$ °C). Unfortunately, in the same conditions, the corresponding double helix is also highly stable ($T_m = 79$ °C), thus preventing an efficient separation of the two strands at 37 °C and consequent G4 formation. Working on the experimental conditions, we did not identify a unique parameter sufficient to fully shift the double helix towards the tetrahelix at physiological temperature. Indeed, KCl, pH and PEG, when take alone, modestly promote the process. Clearly, here we analyzed the effect of a limited number of components in solution, although all of them can partly describe the intracellular environment. Still, our results showed that they can cooperate to facilitate the conversion of the double helix towards alternative foldings. This is actually strictly related to the structural properties of the C-rich strand which can fold into an iM, though under different experimental conditions compared to the G4. Nevertheless, a proper combination of PEG and KCl allows the simultaneous detection of both the tetrahelices at nearly physiological pH values.

Although at the moment no experimental evidences of G4 or iM occurrence within the BRAF gene in living cells are available, these result lead open the possibility that the non-canonical foldings of the herein studied promoter sequence may be significant in the complex physiological environment, thus representing a valuable novel target for the development of innovative anticancer therapies.

Acknowledgments

This work was founded by Universita' degli Studi di Padova (Grant # 60A04-7255 and CPDA147272/14). MLG was founded by CARIPARO.

Appendix A. Supplementary data

Supplementary data associated with this article can be found, in the online version, at http://dx.doi.org/10.1016/j.febslet.2015.06.025.

References

[1] Davis, J.T. (2004) G-quartets 40 years later: from 5′-GMP to molecular biology and supramolecular chemistry. Angew. Chem. Int. Ed. Engl. 43 (6), 668–698.
[2] Patel, D.J., Phan, A.T. and Kuryavyi, V. (2007) Human telomere, oncogenic promoter and 5′-UTR G-quadruplexes: diverse higher order DNA and RNA targets for cancer therapeutics. Nucleic Acids Res. 35 (22), 7429–7455.
[3] Balasubramanian, S., Hurley, L.H. and Neidle, S. (2011) Targeting G-quadruplexes in gene promoters: a novel anticancer strategy? Nat. Rev. Drug Discov. 10 (4), 261–275.
[4] Folini, M. et al. (2011) Telomeres as targets for anticancer therapies. Expert Opin. Ther. Targets 15 (5), 579–593.
[5] Huppert, J.L. et al. (2008) G-quadruplexes: the beginning and end of UTRs. Nucleic Acids Res. 36 (19), 6260–6268.
[6] Lipps, H.J. and Rhodes, D. (2009) G-quadruplex structures: in vivo evidence and function. Trends Cell Biol. 19 (8), 414–422.
[7] Brooks, T.A., Kendrick, S. and Hurley, L. (2010) Making sense of G-quadruplex and i-motif functions in oncogene promoters. FEBS J. 277 (17), 3459–3469.
[8] Huppert, J.L. and Balasubramanian, S. (2007) G-quadruplexes in promoters throughout the human genome. Nucleic Acids Res. 35 (2), 406–413.
[9] Malik, R. and Roy, I. (2011) Making sense of therapeutics using antisense technology. Expert Opin. Drug Discov. 6 (5), 507–526.
[10] Bora, R.S. et al. (2012) RNA interference therapeutics for cancer: challenges and opportunities (review). Mol. Med. Rep. 6 (1), 9–15.
[11] Torti, D. and Trusolino, L. (2011) Oncogene addiction as a foundational rationale for targeted anti-cancer therapy: promises and perils. EMBO Mol. Med. 3 (11), 623–636.
[12] Phan, A.T. et al. (2007) Structure of an unprecedented G-quadruplex scaffold in the human c-kit promoter. J. Am. Chem. Soc. 129 (14), 4386–4392.
[13] Kuryavyi, V., Phan, A.T. and Patel, D.J. (2010) Solution structures of all parallel-stranded monomeric and dimeric G-quadruplex scaffolds of the human c-kit2 promoter. Nucleic Acids Res. 38 (19), 6757–6773.
[14] Mathad, R.I. et al. (2011) C-MYC promoter G-quadruplex formed at the 5′-end of NHE III1 element: insights into biological relevance and parallel-stranded G-quadruplex stability. Nucleic Acids Res. 39 (20), 9023–9033.
[15] Wei, D., Husby, J. and Neidle, S. (2015) Flexibility and structural conservation in a c-KIT G-quadruplex. Nucleic Acids Res. 43 (1), 629–644.
[16] Wei, D. et al. (2012) Crystal structure of a c-kit promoter quadruplex reveals the structural role of metal ions and water molecules in maintaining loop conformation. Nucleic Acids Res. 40 (10), 4691–4700.
[17] Tong, X. et al. (2011) Solution structure of all parallel G-quadruplex formed by the oncogene RET promoter sequence. Nucleic Acids Res. 39 (15), 6753–6763.
[18] Dai, J. et al. (2006) NMR solution structure of the major G-quadruplex structure formed in the human BCL2 promoter region. Nucleic Acids Res. 34 (18), 5133–5144.
[19] Brooks, T.A. and Hurley, L.H. (2010) Targeting MYC expression through G-quadruplexes. Genes Cancer 1 (6), 641–649.
[20] Cogoi, S. and Xodo, L.E. (2006) G-quadruplex formation within the promoter of the KRAS proto-oncogene and its effect on transcription. Nucleic Acids Res. 34 (9), 2536–2549.
[21] Bejugam, M. et al. (2010) Targeting the c-Kit promoter G-quadruplexes with 6-substituted indenoisoquinolines. ACS Med. Chem. Lett. 1 (7), 306–310.
[22] Dai, J. et al. (2011) Solution structure of a 2:1 quindoline-c-MYC G-quadruplex: insights into G-quadruplex-interactive small molecule drug design. J. Am. Chem. Soc. 133 (44), 17673–17680.
[23] Dienstmann, R. and Tabernero, J. (2011) BRAF as a target for cancer therapy. Anticancer Agents Med. Chem. 11 (3), 285–295.
[24] Prahallad, A. et al. (2012) Unresponsiveness of colon cancer to BRAF(V600E) inhibition through feedback activation of EGFR. Nature.
[25] Wei, D. et al. (2013) Crystal structure of a promoter sequence in the B-raf gene reveals an intertwined dimer quadruplex. J. Am. Chem. Soc. 135 (51), 19319–19329.
[26] Day, H.A., Pavlou, P. and Waller, Z.A. (2014) I-Motif DNA: structure, stability and targeting with ligands. Bioorg. Med. Chem. 22 (16), 4407–4418.
[27] Gehring, K., Leroy, J.L. and Gueron, M. (1993) A tetrameric DNA structure with protonated cytosine·cytosine base pairs. Nature 363 (6429), 561–565.
[28] Randazzo, A., Spada, G.P. and da Silva, M.W. (2013) Circular dichroism of quadruplex structures. Top. Curr. Chem. 330, 67–86.
[29] Mergny, J.L. et al. (2005) Thermal difference spectra: a specific signature for nucleic acid structures. Nucleic Acids Res. 33 (16), e138.
[30] Rachwal, P.A. and Fox, K.R. (2007) Quadruplex melting. Methods 43 (4), 291–301.
[31] Mergny, J.-L. et al. (1995) Intramolecular folding of pyrimidine oligodeoxynucleotides into an i-DNA motif. J. Am. Chem. Soc. 117 (35), 8887–8898.
[32] Brazier, J.A., Shah, A. and Brown, G.D. (2012) I-motif formation in gene promoters: unusually stable formation in sequences complementary to known G-quadruplexes. Chem. Commun. (Camb.) 48 (87), 10739–10741.
[33] Dhakal, S. et al. (2010) Coexistence of an ILPR i-motif and a partially folded structure with comparable mechanical stability revealed at the single-molecule level. J. Am. Chem. Soc. 132, 8991–8997.
[34] Dettler, J.M. et al. (2010) Biophysical characterization of an ensemble of intramolecular i-motifs formed by the human c-MYC NHE III1 P1 promoter mutant sequence. Biophys. J. 99 (2), 561–567.
[35] Miyoshi, D., Nakao, A. and Sugimoto, N. (2002) Molecular crowding regulates the structural switch of the DNA G-quadruplex. Biochemistry 41 (50), 15017–15024.
[36] Buscaglia, R. et al. (2013) Polyethylene glycol binding alters human telomere G-quadruplex structure by conformational selection. Nucleic Acids Res. 41 (16), 7934–7946.
[37] Sharma, V.R. and Sheardy, R.D. (2013) The human telomere sequence, (TTAGGG)4, in the absence and presence of cosolutes: a spectroscopic investigation. Molecules 19 (1), 595–608.
[38] Rajendran, A., Nakano, S. and Sugimoto, N. (2010) Molecular crowding of the cosolutes induces an intramolecular i-motif structure of triplet repeat DNA oligomers at neutral pH. Chem. Commun. (Camb.) 46 (8), 1299–1301.
[39] Heddi, B. and Phan, A.T. (2011) Structure of human telomeric DNA in crowded solution. J. Am. Chem. Soc. 133, 9824–9833.
[40] Cui, J. et al. (2013) The effect of molecular crowding on the stability of human c-MYC promoter sequence I-motif at neutral pH. Molecules 18 (10), 12751–12767.
[41] Bhavsar-Jog, Y.P. et al. (2014) Epigenetic modification, dehydration, and molecular crowding effects on the thermodynamics of i-motif structure formation from C-rich DNA. Biochemistry 53 (10), 1586–1594.